Journal of Organometallic Chemistry, 335 (1987) 255–268
Elsevier Sequoia S.A., Lausanne – Printed in The Netherlands

Synthesis, characterization, and electrochemistry of the mono- and bi-dentate xanthate complexes η^5-$C_5R_5Fe(CO)(\eta^1$-$SC(S)OEt)L$ and η^5-$C_5R_5Fe(\eta^2$-$S_2COEt)L$ ($R = H, Me; L = PBu_3, PPh_3, P(OEt)_3, P(OPh)_3$)

M. Morán, I. Cuadrado, J.R. Masaguer,
Departamento de Química, Facultad de Ciencias C-VIII, Universidad Autónoma de Madrid, Cantoblanco, 28049, Madrid (Spain)

and J. Losada
Departamento de Química Inorgánica y Analítica, E.T.S. de Ingenieros Industriales, Universidad Politécnica de Madrid (Spain)

(Received April 21st, 1987)

Abstract

The mixed carbonyl-phosphorus ligand monodentate xanthate complexes η^5-$C_5H_5Fe(CO)(\eta^1$-$SC(S)OEt)L$ (**5a–5d**), can be conveniently obtained by treatment of the dicarbonyl compound η^5-$C_5H_5Fe(CO)_2(\eta^1$-$SC(S)OEt)$ (**1**) with the appropriate phosphine or phosphite ligand L (PBu_3, PPh_3, $P(OEt)_3$, $P(OPh)_3$). In contrast, similar reactions between the analogous pentamethylcyclopentadienyl complex η^5-$C_5Me_5Fe(CO)_2(\eta^1$-$SC(S)OEt)$ (**2**) and the same phosphorus ligands L give not only the substituted complexes η^5-$C_5Me_5Fe(CO)(\eta^1$-$SC(S)OEt)L$ (**6a–6d**), but also the monocarbonyl-bidentate xanthate complex η^5-$C_5Me_5Fe(CO)(\eta^2$-$S_2COEt)$ (**4**), with the ratio of these two types of products dependent on the ligand L. UV photolysis of the monodentate xanthate series of complexes **5** and **6** gives the complexes η^5-$C_5R_5Fe(\eta^2$-$S_2COEt)L$ ($R = H$ (**7a–7d**); $R = Me$ (**8a–8d**). The complexes **5a–5d** and **6a–6d** undergo one-electron oxidation by an EC mechanism leading to the corresponding bidentate xanthate complexes **7a–7d** and **8a–8d**. For **5c**, **5d** and **6d** formation of the cationic species $[\eta^5$-$C_5R_5Fe(CO)L]^+$ ($R = H$ and Me) is also observed.

Introduction

We have previously described the different types of behaviour displayed by the ligands bis(dialkylphosphorothionyl) disulphides $[SP(S)R_2]_2$ ($R = Et$, OEt, and

0022-328X/87/$03.50

O^{i}Pr) [1,2]. These disulphides react with $[\eta^5\text{-}C_5R_5Fe(CO)_2]_2$ (R = H and Me) to give the dithiophosphate complexes $\eta^5\text{-}C_5R_5Fe(CO)_2(\eta^1\text{-}SP(S)R_2)$, in which the ligand $SP(S)R_2$ is bonded to the iron atom in monodentate fashion [1]. In the reactions of these ligands with vanadocene, oxidation takes place to give the stable vanadium(IV) complexes $[(\eta^5\text{-}C_5H_5)_2V(\eta^2\text{-}S_2PR_2)]^+[S_2PR_2]^-$, in which the dithiophosphate ligands show two distinct modes of coordination, bidentate and ionic [2].

We recently reported the preparation, characterization and electrochemical behaviour of the dicarbonyl monodentate xanthate complexes $\eta^5\text{-}C_5R_5Fe(CO)_2(\eta^1\text{-}SC(S)OEt)$ (R = H (**1**); R = Me (**2**)), involving oxidative cleavage of the Fe–Fe bond in the dimers $[\eta^5\text{-}C_5R_5Fe(CO)_2]_2$ (R = H and Me), and homolytic fragmentation of the S–S bond in the diethyldixantogen $[SC(S)OEt]_2$ [3]. We also examined the reactivity of the free sulfur atom in the η^1-xanthate ligand in complexes **1** and **2**, and we induced chelation by UV photolysis to give the new monocarbonyl bidentate xanthate complexes $\eta^5\text{-}C_5R_5Fe(CO)(\eta^2\text{-}S_2COEt)$ (R = H (**3**); R = Me (**4**)). We have now completed a more detailed investigation of the reactivity of complexes **1** and **2**, and describe here the reactions between these complexes and some phosphorus donor ligands L (PBu_3, PPh_3, $P(OEt)_3$ and $P(OPh)_3$) to give the mixed monocarbonylphosphine-η^1-xanthate complexes $\eta^5\text{-}C_5R_5Fe(CO)(\eta^1\text{-}SC(S)OEt)L$, (**5a–5d**), and (**6a–6d**). We have also found that replacement of CO and subsequent chelation of the η^1-xanthate ligand in both **5** and **6** be brought about by UV photolysis, to give the compounds $\eta^5\text{-}C_5R_5Fe(\eta^2\text{-}S_2COEt)$, (**7a–7d**) and (**8a–8d**). We also present details of the electrochemistry of complexes **5a–5d** and **6a**, **6c** and **6d**.

Results and discussion

The reactions between the dicarbonyl monodentate xanthate complex $\eta^5\text{-}C_5H_5Fe(CO)_2(\eta^1\text{-}SC(S)OEt)$ (**1**) and phosphine or phosphite ligands L in n-heptane at 85–90 ° C, give high yields of the mixed monocarbonylphosphorus ligand complexes $\eta^5\text{-}C_5H_5Fe(CO)(\eta^1\text{-}SC(S)OEt)L$ (L = PBu_3 (**5a**); PPh_3 (**5b**); $P(OEt)_3$ (**5c**); $P(OPh)_3$ (**5d**)) (Scheme 1). After purification by column chromatography the new complexes **5a–5d** are obtained as red-orange or yellow crystalline diamagnetic solids, which can be handled in air for several hours without significant decomposition but which dissolve in polar solvents to give air sensitive solutions. In all cases, the progress of the reactions was monitored by IR spectroscopy. For all four compounds, large crystals were obtained by recrystallization from cyclohexane or a cyclohexane/n-hexane (1/1) mixture.

The behaviour of its analogous pentamethylcyclopentadienyldicarbonyl η^1-xanthate complex, $\eta^5\text{-}C_5Me_5Fe(CO)_2(\eta^1\text{-}SC(S)OEt)$ (**2**), is significantly different [4*]. Thus, under the same conditions (n-heptane, 85–90 ° C), reactions of **2** with the same phosphorus ligands L give not only the mixed substituted carbonyl-phosphine or -phosphite complexes $\eta^5\text{-}C_5Me_5Fe(CO)(\eta^1\text{-}SC(S)OEt)L$, (L = PBu_3 (**6a**); $P(OEt)_3$ (**6c**); $P(OPh)_3$ (**6d**)), but also the monocarbonyl bidentate xanthate complex, $\eta^5\text{-}C_5Me_5Fe(CO)(\eta^2\text{-}S_2COEt)$ (**4**). The yields of the complexes **6a**, **6c**, **6d** depend on the ligand L, viz.: **6a** (ca. 60%), **6c** (ca. 55%), and **6d** (ca. 15%). Furthermore, our

---

* Reference numbers with asterisks indicate notes in the list of references.

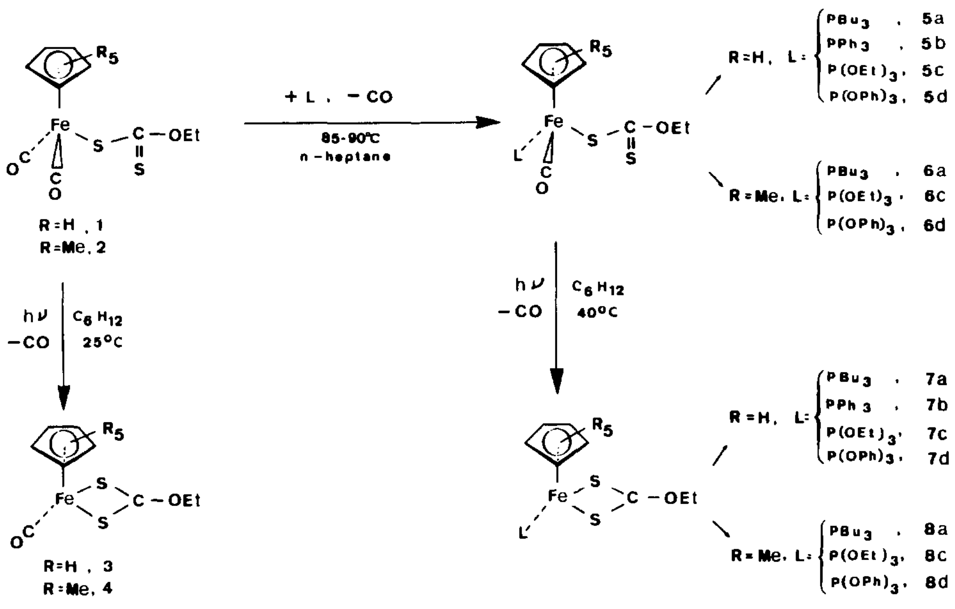

Scheme 1

attempts to obtain the complex η^5-$C_5Me_5Fe(CO)(\eta^1$-$SC(S)OEt)(PPh_3)$ (**6b**) were unsuccessful even under forcing conditions (higher temperatures or/and long reaction times), only the chelated xanthate complex η^5-$C_5Me_5Fe(CO)(\eta^2$-$S_2COEt)$ (**4**) being isolated. This is probably due to stereoelectronic reasons (greater bulk and/or lower electron releasing effects of the L ligands). The formation of the complex with PPh_3, which is the bulkiest of the phosphorus ligands studied (cone angle θ, 145° [5]) may be prevented by steric hindrance arising from the greater size of the η^5-C_5Me_5 ring (the cone angle for η^5-C_5H_5 is 110°, whereas that for η^5-C_5Me_5 ring is 142° [6]).

Complex **4** was identified by comparaison of its analytical and spectroscopic data with those of an authentic sample [3]. The formation of **4** is probably due to the greater tendency toward chelation of the η^1-xanthate ligand in complexes containing the C_5Me_5 ring arising from the higher electron donor ability of η^5-C_5Me_5, which increases the nucleophilic character of the uncoordinated sulfur atom in the η^1-$SC(S)OEt$ ligand. Similar preference toward chelation has been found in carbonyliron η^1-dithiocarbamate complexes with η^5-C_5H_5 and η^5-C_5Me_5 rings [7,8a].

In these reactions, the separation of the two products **4** and **6** was accomplished by column chromatography (neutral alumina) with cyclohexane and cyclohexane/tetrahydrofuran mixtures as eluents. The substituted mixed carbonylphosphorus ligand complexes (**6**) were obtained as red crystals (**6a**) or orange or red-brown oils **6c** and **6d**.

We also investigated the reactivity of the free sulfur atom of the η^1-xanthate ligand in the new η^5-$C_5R_5Fe(CO)(\eta^1$-$SC(S)OEt)L$ complexes and found that UV irradiation of cyclohexane solutions of **5a–5d** and **6a**, **6c** and **6d** at 40 °C results in immediate reaction as evidenced by a colour change to violet. Monitoring of the reaction by IR spectroscopy revealed that the strong carbonyl band due to the

Table 1

Characteristic IR data for the iron-xanthate complexes [a]

Complex	ν(C–O–C′)	ν(C=S)	ν(CO)		K_{CO}^{b}
			CH_2Cl_2	n-Heptane	
1	1185vs	1042vs	2042vs		16.50
			1998vs		0.38
2	1180vs	1042vs	2021vs		16.13
			1973vs		0.37
5a	1176vs	1039vs	1949vs	1954vs	15.34
				1962sh	
5b	1175vs	1038vs	1965vs	1960vs	15.43
5c	1172vs	1038vs	1968vs	1966vs	15.64
				1976sh	
5d	1173vs	1039vs	1986vs	1989vs	1592
6a	1170vs	1036vs	1926vs	1939vs	14.98
				1930sh	
6c	1164vs	1039vs	1940vs	1943vs	15.20
				1953sh	
6d	1169vs	1035vs	1962vs	1966vs	15.54
				1979sh	
7a	1219vs	1030s			
7b	1220vs	1029s			
7c	1222vs	1027s			
7d	1222vs	1028s			
8a	1225vs	1026s			
8c	1223vs	1028s			
8d	1225vs	1025s			

[a] In cm^{-1}. [b] K_{CO} in mdyn.A^{-1}. Values for CH_2Cl_2 solutions. Determinated by the method of Cotton and Kraihanzel [20].

starting carbonyliron η^1-xanthate complexes **5** and **6** gradually decreases and completely disappears in 1–5 h. After purification by chromatography, the complexes **7a–7d** and **8a–8d** (Scheme 1) were isolated as red-violet, very air-sensitive solids or oils. The extremely high air-sensitivity of these complexes is consistent with their electrochemical behaviour, which reveals relatively low values of the redox potential for the reversible oxidation. These reactions also illustrate the nucleophilic nature of the uncoordinate sulfur atom in the monodentate xanthate complexes **5a–5d** and **6a**, **6c** and **6d**.

The coordination mode of the xanthate ligand, which is monodentate in the η^5-$C_5R_5Fe(CO)(\eta^1$-SC(S)OEt)L series **5a–5d** and **6a**, **6c** and **6d**, but bidentate in complexes η^5-$C_5R_5Fe(\eta^2$-$S_2COEt)L$ (**7a–7d** and **8a–8d**), can be inferred from the IR spectra. For both coordination modes, the xanthate ligands exhibit three bands in the 1250–1000 cm^{-1} region, which are related to the vibrations of the SC(S)OR group and, assigned to ν(COEt), ν(CO), and ν(CS) vibrations [9–11]. For **5a–5d**, **6a**, **6c**, **6d**, **7a–7d** and **8a–8d**, the characteristic xanthate bands are listed in Table 1. The band assigned to ν(COC) appears at higher frequencies (ν(COC) ca. 1230–1210 cm^{-1}) in complexes η^5-$C_5R_5Fe(\eta^2$-$S_2COEt)L$ than in η^5-$C_5R_5Fe(CO)(\eta^1$-SC(S)OEt)L (ν(COC) ca. 1180 cm^{-1}). Likewise, the ν(C=S) values are higher for complexes **5** and **6** than for the complexes **7** and **8** because in these the CS bond has less double bond character. The positions of the characteristic bands of the monoor bi-dentate xanthate compounds are consistent with those for other organometallic titanium and iron complexes with the same ligands [3,12,13].

The greater electron donor ability of η^5-C_5Me_5 than of η^5-C_5H_5 is reflected in the ν(CO) values, which are lower in **6a**, **6c** and **6d** than in **5a–5d**. There is a corresponding decrease in the values of carbonyl force constants, K(CO), as indicated in Table 1.

In some of the monocarbonyl complexes, the ν(CO) absorptions in the IR spectra, recorded for n-heptane or cyclohexane solutions, shows two clearly resolved bands (Table 1), both due to ν(CO) vibrations of the sole carbonyl ligand, and it is clear that these compounds exhibit some form of isomerism. However, in more polar solvents such as CH_2Cl_2, only one broad absorption appears. There are two possible origins of this isomerism: (a) restricted rotation about the Fe–P bond, with formation of eclipsed and staggered isomers, and (b) restricted rotation within the P–O–C group of the ligand, which gives rise to two conformational isomers of $P(OR)_3$, and thus, two isomers of the complexes. This last possibility of only **5c**, **5d** and **6c**, **6d** complexes, but we have observed isomerism in complexes with PBu_3 and PPh_3 ligands, and so it is likely that the isomerism arises from both of the effects (a) and (b). Similar behaviour is shown by a wide variety of complexes η^5-$C_5H_5M(CO)LX$ (L = $P(OR)_3$, PPh_3; M = Fe, Mn, Cr, Mo) [14], but is not observed in similar complexes with PBu_3 [14].

Replacement of a carbonyl group in **1** and **2** by a weaker π-acceptor phosphorus ligand PR_3 or $P(OR)_3$ [15–18] results in an increase in the π-donation fron iron to the remaining carbonyl group in complexes **5a–5d** and **6a**, **6c** and **6d**. This leads to a decrease in ν(CO) and force constants, as it is shown by the data in Table 1.

Analysis of the ν(CO) values for each of the two series of complexes **5a–5d** and **6a**, **6c** and **6d** shows that there is an important variation (about 15 to 40 cm^{-1}) in the ν(CO) frequency with the phosphorus ligand L. Thus, lower ν(CO) values are found in complexes with PBu_3 and higher values for $P(OPh)_3$ (see Table 1). This can be rationalized in terms of the different electronic effects of the phosphine or

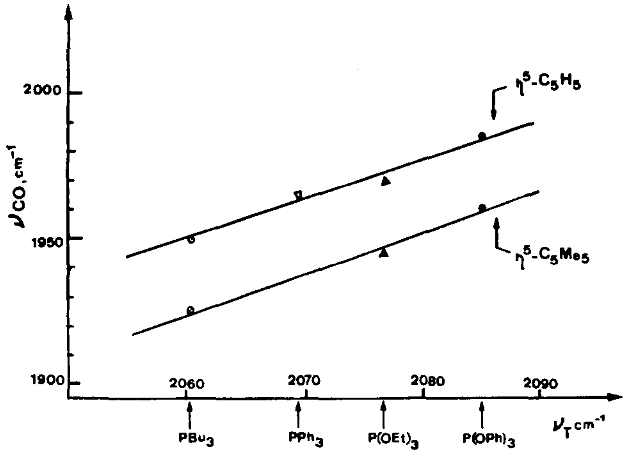

Fig. 1. Plot of ν(CO) against the Tolman electronic parameter ν_T, for the complexes η^5-$C_5R_5Fe(CO)(\eta^1$-SC(S)OEt)L, (R = H: (**5a–5d**; R = Me: (**6a,6c,6d**); L = PBu_3, PPh_3, $P(OEt)_3$ and $P(OPh)_3$.

phosphite ligands [5,19]. For **5a–5d**, **6a**, **6c** and **6d** it is possible to discern a relationship between ν(CO) and the Tolman electronic parameter [5] (indicated here by ν_T (cm^{-1})), as observed for a variety of a monosubstituted transition metal carbonyl complexes [5]. As shown in Fig. 1, there is a linear relationship between ν(CO) and ν_T with the lower ν(CO) values in complexes with PBu_3, which has the lowest ν_T value [5].

Electrochemical studies

Figures 2 and 3 show typical cyclic voltammograms (CV) of the studied complexes in CH_3CN (0.1 *M* $[NBu_4][PF_6]$). They are qualitatively the same with dichloromethane as solvent. The cyclic voltammograms are characterized by an anodic peak, A, and the corresponding cathodic peak, A′, the intensity of which varies in the reverse scan (Table 2). The CV of **5c**, **5d**, and **6d** do not show this cathodic peak, even at high scan rates (5 V s^{-1}). The ratio i_c/i_a (Table 2) is less than units, indicating that an irreversible chemical reaction is coupled with the electrode process. From this ratio values it follows that the stability of the cation formed is very dependent on the phosphorus ligand and on the ring substituents [21*]. However, at low temperatures (−30 °C) the cyclic voltammograms of all the complexes exhibit well-defined cathodic wave on the reverse scan, with a ratio i_c/i_a of 1 and E_p close to 60 mV (Fig. 2c).

The electron transfers are diffusion controlled, with anodic current function ($i_{p,a}/v^{1/2}$) independent of the scan rate (v) over the range of scan rates used. Potentiostatic coulometry and comparisons of limiting currents obtained from rotating disk electrode (RDE) voltammograms for **5a–5d** and **6a**, **6c** and **6d**, with those for ferrocene indicate a one-electron exchange in these oxidation steps.

In the case of the complexes **5a**, **5b**, **6a** and **6c** the voltammograms (Fig. 2) display another cathodic peak, B′, at more negative potentials. In addition, the second and subsequent scans show a new coupled oxidation peak, B, with ΔE_p ca. 60 mV. In the multicyclic voltammograms of **5c**, **5d**, and **6d**, this couple, presumably corresponding to a reversible system, is poorly defined (Fig. 3). However, for these complexes an additional irreversible reduction peak C′, is observed at more cathodic potentials (Table 2), and remains irreversible even at high scan rates (5 V s^{-1}). At lower temperatures, none of these supplementary waves, B, B′, and C′, are observed.

All the cyclic voltammograms of η^5-$C_5R_5Fe(\eta^2$-$S_2COEt)L$ (**7a–7d** and **8a–8d**) show a pair of anodic and cathodic peaks (Fig. 2a). These electrochemical processes are diffusion controlled, with the anodic current function independent of the scan rates, and a ratio of anodic to cathodic current, i_a/i_c, of 1. Potentiostatic coulometry and comparisons of the limiting current obtained from RDE voltammograms with those for ferrocene indicate one-electron transfers. The potential values of these peaks match the voltages of the B/B′ couple in the multicyclic voltammograms (Fig. 2 and Table 2).

In contrast the CV's of the solutions obtained from exhaustive electrolysis of complexes **5a**, **5b**, **6a** and **6c** show only the peaks B and B′ [25*]. This suggest that the CO group is released with the xanthate ligand becoming bidentate. However, in the case of complexes **5c**, **5d** and **6d**, cyclic voltammograms of the solutions obtained

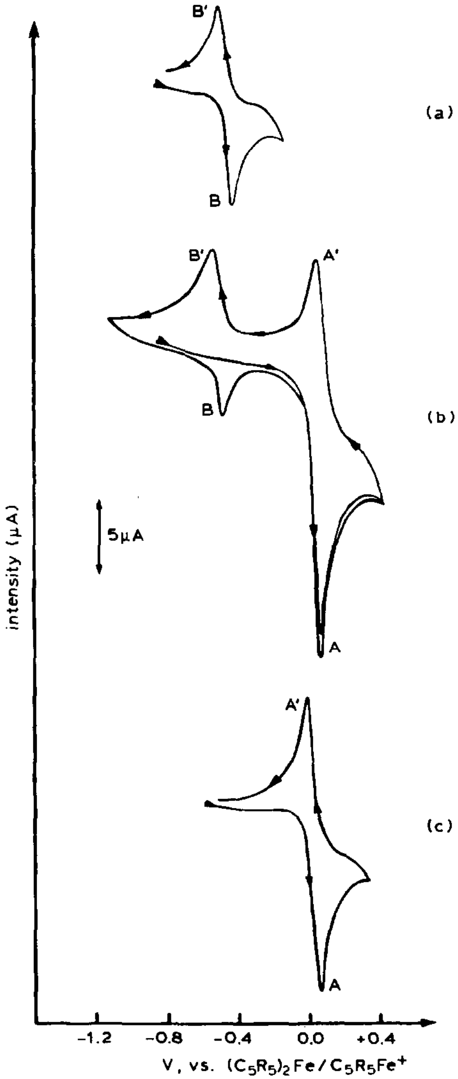

Fig. 2. Cyclic voltammograms, in CH_3CN solution, at a carbon glassy electrode for: (a) η^5-$C_5H_5Fe(\eta^2$-$S_2COEt)(PBu_3)$, scan rate 0.2 V s^{-1}; (b) η^5-$C_5H_5Fe(CO)(\eta^1$-$SC(S)OEt)(PBu_3)$, scan rate 0.2 V s^{-1}; (c) η^5-$C_5H_5Fe(CO)(\eta^1$-$SC(S)OEt)(PBu_3)$, at −30 °C, scan rate 0.2 V s^{-1}.

from exhaustive controlled potential electrolysis include the less intense wave C′ in addition to the couple B/B′.

The peak C′ is probably due to the reduction of the $[\eta^5$-$C_5R_5Fe(CO)L]^+$ cations, L = $P(OEt)_3$, $P(OPh)_3$, arising from the oxidation of the original compounds followed by the loss of the xanthate ligand [26*]. The formation of these cations is confirmed by the IR spectra. After exhaustive bulk electrolysis of the η^5-$C_5H_5Fe(CO)(\eta^1$-$SC(S)OEt)P(OPh)_3$, the IR spectra show a band at 2004 cm^{-1}, characteristic of the cation $[\eta^5$-$C_5H_5Fe(CO)P(OPh)_3]^+$ [27], the stability of which has been explained in terms of the cone angle and π-character of the triphenylphos-

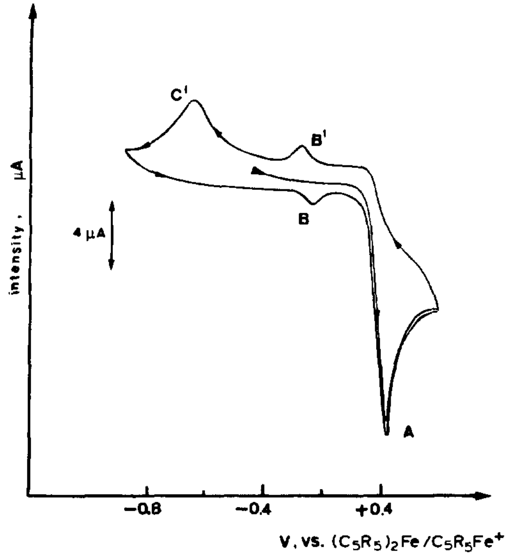

Fig. 3. Cyclic voltammogram in CH_3CN solution at a carbon glassy electrode for η^5-$C_5H_5Fe(CO)(\eta^1$-$SC(S)OEt)(P(OPh)_3)$; scan rate 0.3 V s^{-1}.

phite ligand. Analogous behaviour is found for complexes **5c** and **6d**, the IR spectra of which show bands at 1997 and 1990 cm^{-1} corresponding to the cations $[\eta^5$-$C_5R_5Fe(CO)P(OEt)_3]^+$ R = H and Me.

It has been reported that the cation $[\eta^5$-$C_5H_5Fe(CO)PPh_3]^+$ is much less stable than the triphenylphosphite analogue [27], and this accounts for the fact that it is

Table 2

Cyclic voltammetric [a] data for the complexes at 200 mV s^{-1}

Compounds	ΔHNP [b]	Solvent	E_p(A)	E_p(A′)	i_c/i_a	$E_{1/2}$(A/A′) [c]	$E_{1/2}$(B/B′) [d]	E_p(C′)
5a	131	CH_3CN	+0.12	+0.06	0.44	+0.07	−0.53	
		CH_2Cl_2	+0.14	+0.07	0.46	+0.08	−0.54	
5c	420	CH_3CN	+0.22	+0.15	0	+0.16	−0.44	−0.98
		CH_2Cl_2	+0.28	+0.17	0	+0.18	−0.42	−0.92
5b	573	CH_3CN	+0.30	+0.23	0	+0.24	−0.37	
		CH_2Cl_2	+0.33	+0.26	0	+0.27	−0.35	
5d	875	CH_3CN	+0.42	+0.35	0	+0.36	−0.17	−0.65
		CH_2Cl_2	+0.44	+0.37	0	+0.38	−0.14	−0.63
6a		CH_3CN	−0.02	−0.08	0.73	−0.04	−0.81	
		CH_2Cl_2	0.00	−0.06	0.76	−0.01	−0.79	
6c		CH_3CN	+0.05	−0.02	0.82	+0.04	−0.57	
		CH_2Cl_2	+0.08	+0.01	0.84	+0.06	−0.54	
6d		CH_3CN	+0.20	+0.13	0	+0.14	−0.42	−0.80
		CH_2Cl_2	+0.23	+0.16	0	+0.17	−0.40	−0.77

[a] At glassy carbon electrode. Peak potentials relative to the $Cp_2Fe/CpFe^+$ couple. [b] Basicity of the phosphorus ligand, ΔHNP = half-neutralization potential relative to that for *N,N′*-diphenylquamidine in nitromethane. Greater basicity is indicated by smaller ΔHNP values. [c] at −30 °C. [d] For the (**7a**–**7d**)/[(**7a**–**7d**)]$^+$ and (**8a**–**8d**)/[(**8a**–**8d**)]$^+$ couples (see text). [d] The ratio values i_c/i_a are unity in all cases.

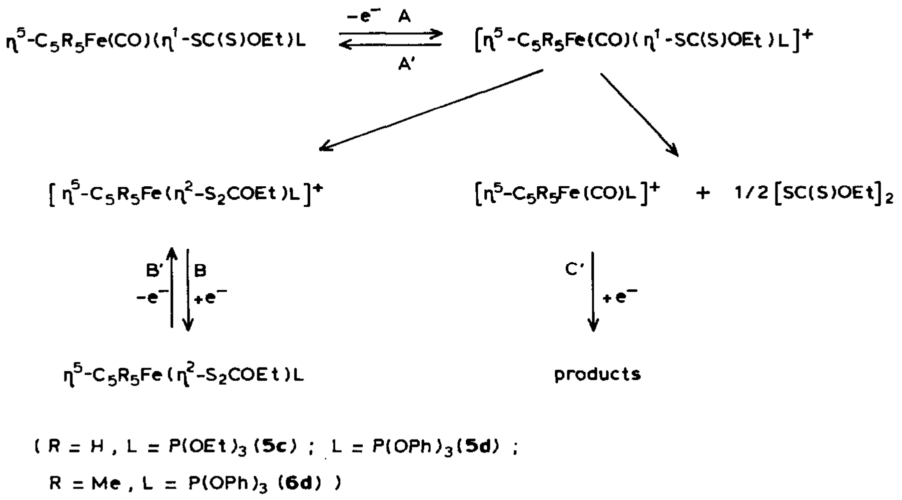

Scheme 2

not formed in the cyclovoltammetric experiments. The results suggest that in the case of complexes **5c**, **5d**, and **6d** the final products of oxidation arise from two separate reaction paths, although the elimination of the xanthate ligand seems to be the more important.

The mechanism of anodic oxidation of the complexes is summarized in Scheme 2.

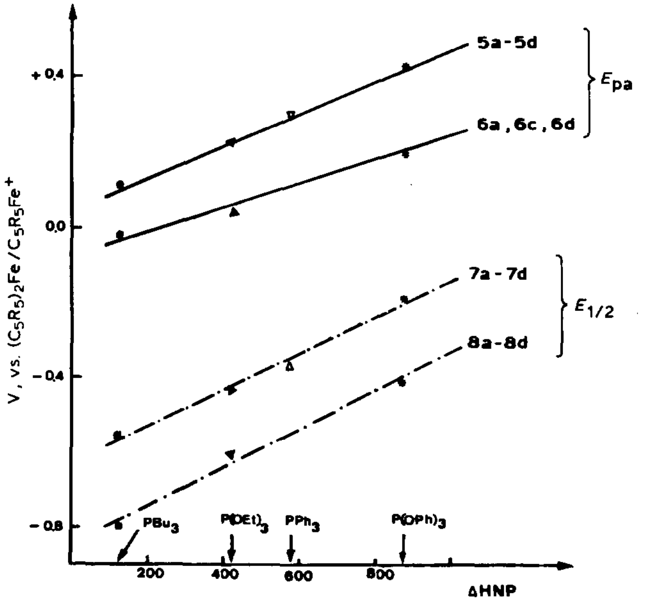

Fig. 4. Variation of the ΔHNP (half-neutralization potential) with the anodic oxidation potential $E_{p,a}$ or $E_{1/2}$ for the complexes η^5-C$_5$R$_5$Fe(CO)(η^1-SC(S)OEt)L, (**5a–5d**), (**6a,6c,6d**) and η^5-C$_5$R$_5$Fe(η^2-S$_2$COEt)L, (**7a–7d**), (**8a–8d**).

A similar $\overrightarrow{E}C\overleftarrow{E}$ process is known for chelation of the dithiocarbamate ligand η^5-C_5H_5Fe-η^1-SC(S)NMe_2 with CO loss [8b,c].

As shown in Table 2, the greater electron-donor ability of C_5Me_5 results in a shift for the anodic peaks to less positive potentials by 150 mV on substitution of H for Me, in keeping with the significant inductive effect of the Me groups.

The oxidation potentials depend on the basicity of the phosphorus ligand. A plot of $E_{p,a}$ for the complexes against ΔHNP of the phosphorus ligand L (Fig. 4) is linear, which indicates that the oxidation potential is predominantly influenced by the ability of the ligand to transfer the σ-electron to the metal atom. An increase of electron density on the metal atom would then shift the $E_{p,a}$ to less positive potentials. Similar results were found for **7a–7d** and **8a–8d**.

Experimental

General data

All reactions and manipulations were carried out by Schlenk techniques under oxygen-free nitrogen. Tetrahydrofuran was distilled from sodium benzophenone ketyl under nitrogen immediately before use. Dichloromethane, n-heptane, cyclohexane and acetonitrile were distilled from phosphorus pentoxide under nitrogen. Triphenylphosphine (Fluka) was recrystallized from ethanol/ether. Tri-n-butylphosphine, triethylphosphite, and triphenylphosphite (Fluka) were used as received. The complexes η^5-$C_5R_5Fe(CO)_2$(η^1-SC(S)OEt) (R = H (**1**) and R = Me (**2**)), were prepared from $[\eta^5\text{-}C_5R_5Fe(CO)_2]_2$, and $[SC(S)OEt]_2$ as previously described [3]. Chromatographic separations and purifications were carried out with a neutral alumina (Fluka) (2 × 30 cm) column.

Infrared spectra were recorded with a Nicolet 5 DX FT-IR spectrometer using Nujol and hexachlorobutadiene mulls, between CsI windows. The solution spectra (CH_2Cl_2, n-heptane, or cyclohexane), were examined in a 0.1 mm liquid cell with KBr windows. In all cases the solvent absorption was substracted by use of the software of the spectrophotometer. The ^1H and ^{13}C NMR spectra were recorded with a Bruker WH-200-5Y (200 MHz) FT mode spectrometer. The NMR chemical shifts are reported in parts per million δ (ppm) relative to internal Me_4Si.

Cyclic voltammetric measurements were carried out with a Metrohm VA-Scanner in conjuction with a Metrohm VA-detector and a Linseis LY-17100 X-Y recorder. Fast scan cyclic voltammograms are recorded on a Hitachi VC-6015 digital storage oscilloscope. The coulometric experiments were carried out with a Beckman Electroscan 30 instrument. The electrochemical measurements were performed in a three-electrode cell, with a glassy carbon working electrode, a platinum wire auxiliary electrode, and an aqueous satured calomel electrode (SCE) in CH_3CN and CH_2Cl_2. The reference electrode was separated from the test solution by Vycor frit and a bridge of $[N\text{-}n\text{-}Bu_4][PF_6]$ (0.1 mol dm^{-3}) in the corresponding solvent. The peak potentials are given relative to the ferrocene/ferricinium couple.

A sample solution containing a metal complex (10^{-3} *M*) and a supporting electrolyte, (0.1 *M*), was degassed with purified nitrogen prior to the measurements. For bulk electrolyses, the working electrode was a platinum mesh electrode.

Preparation of complexes

The synthesis of one example of each of the series of complexes η^5-

Table 3

Preparative details and physical and analytical data for complexes η^5-C_5R_5Fe(CO)(η^1-SC(S)OEt)L and η^5-C_5R_5Fe(η^2-S_2COEt)L (R = H and Me) [a]

Complex	T (°C)	t (h)	Yield (%)	Colour	Analysis (Found(calcd.) (%))		
					C	H	Fe
5a	85–90	1	65	red	53.95	7.80	11.50
					(53.38)	(7.89)	(11.82)
5b	85–90	2	60	orange	59.50	4.65	10.25
					(60.91)	(4.73)	(10.49)
5c	85–90	2	80	orange	40.86	5.83	12.50
					(41.29)	(5.78)	(12.80)
5d	85–90	4	85	yellow	55.90	4.68	9.50
					(55.37)	(4.34)	(9.62)
6a	85–90	10	60	red	56.95	8.43	10.15
					(57.55)	(8.73)	(10.19)
6c	85–90	20	55	orange [b]	47.96	6.19	10.98
					(47.43)	(6.97)	(11.03)
6d	85–90	20	15	red-brown [b]	58.95	5.95	8.12
					(59.08)	(5.42)	(8.58)
7a	40	1	70	violet	53.90	12.95	8.10
					(54.05)	(12.61)	(8.33)
7b	40	3	67	violet	61.25	5.78	10.95
					(61.90)	(5.63)	(11.11)
7c	40	1	80	red-violet [b]	41.95	6.78	13.10
					(41.17)	(6.12)	(13.72)
7d	40	3	60	red-violet	57.80	4.80	10.10
					(57.14)	(4.58)	(10.25)
8a	40	1	50	violet [b]	58.95	9.70	10.15
					(58.36)	(9.14)	(10.89)
8c	40	5	65	violet [b]	47.10	7.60	11.55
					(47.69)	(7.32)	(11.71)
8d	40	5	40	red-violet [b]	59.10	5.75	9.50
					(59.80)	(5.62)	(9.00)

[a] η^5-C_5R_5: R = H and R = Me; L = PBu_3, PPh_3, $P(OEt)_3$, and $P(OPh_3)$. [b] Oil.

C_5H_5Fe(CO)(η^1-SC(S)OEt)L, (**5a–5d**); η^5-C_5Me_5Fe(CO)(η^1-SC(S)OEt)L, (**6a,6c,6d**), and η^5-C_5R_5Fe(η^2-S_2COEt)L, (R = H (**7a–7d**), (R = Me (**8a–8d**)), L = PBu_3, PPh_3, $P(OEt)_3$ and $P(OPh)_3$, is described in detail. The preparations of the other complexes were essentially similar, and their physical and analytical data are given in Table 3.

Synthesis of η^5-C_5H_5Fe(CO)(η^1-SC(S)OEt)(PBu_3) (5a). A degassed and stirred n-heptane solution (40 ml) of 0.5 g (1.7 mmol) of η^5-$C_5H_5Fe(CO)_2$(η^1-SC(S)OEt) (**1**) was kept at 35 °C under oxygen-free nitrogen, until the solid had dissolved. To the red solution was added tri-n-butylphosphine (0.7 g, 3.5 mmol). The stirred mixture was kept at 85–90 °C and the progress of the reaction was monitored by IR spectroscopy, which revealed that the two strong carbonyl absorptions due to the initial complex (**1**), at 2041 and 1997 cm^{-1}, gradually diminished in intensity; and at the same time a new absorption at 1954 cm^{-1} appeared and grew. After 1 h, the initial higher ν(CO) bands had completely disappeared, and, only one strong band corresponding to the mixed monocarbonyl-tributylphosphine complex (**5a**) was present. The n-heptane solution was allowed to cool the filtered, and the solvent was removed in vacuo. The residue was dissolved in cyclohexane and transferred to a chromatographic column. Elution with cyclohexane gave a single, orange-red, band. The volume of the solution was reduced to 15 ml, n-hexane was added, and the mixture was kept at −50 °C to give red-orange crystals of η^5-C_5H_5Fe(CO)(η^1-SC(S)(OEt)PBu$_3$ (**5a**), in 65% yield. The compound can be recrystallized from warm cyclohexane or a cyclohexane/hexane mixture. ^{1}H NMR (δ (ppm), $CDCl_3$): 1.52(t, 3H, CH_3); 1.30–0.6(br, 6H, CH_3); 4.46(q, 2H, CH_2); 5.04(s, 5H, C_5H_5); ^{13}C NMR (δ, $CDCl_3$): 13.50(s, CH_3); 13.95(s, CH_3); 24.20(d), 25.63(d), 27.55(d)(CH_2); 69.05(s, CH_2); 82.31(s, C_5H_5); 219.62, 220.00(s, CO, CS).

5b: ^{1}H NMR (δ (ppm), $CDCl_3$): 1.51(t, 3H, CH_3); 4.50(q, 2H, CH_2); 5.10(s, 5H, C_5H_5); 7.45(m, br, 15H, C_6H_5). ^{13}C NMR (δ (ppm), $CDCl_3$): 14.81(s, CH_3); 69.40(s, CH_2); 84.33(s, C_5H_5); 125.00(d, *m*-C_6H_5); 127.20(d, *o*-C_6H_5); 130.35(d, *p*-C_6H_5); 219.74(s, CO)

5c: ^{1}H NMR (δ (ppm), $CDCl_3$): 1.52(m, 6H, CH_3); 4.35(m, 4H, CH_2); 5.05(s, 5H, C_5H_5). ^{13}C NMR (δ (ppm), $CDCl_3$): 13.80(s, CH_3); 15.80(d, CH_3, *J*(PC) 6.1 Hz); 61.30(d, CH_2, *J*(PC) 5.2 Hz); 69.05(s, CH_2); 83.45(s, C_5H_5); 218.20, 219.70(s, CO, CS).

5d: ^{1}H NMR (δ (ppm), $CDCl_3$): 1.52(t, 3H, CH_3); 4.71(m, 2H, CH_2); 5.11(s, 5H, C_5H_5); 7.40(m, 15H, C_6H_5). ^{13}C NMR (δ (ppm), $CDCl_3$): 14.20(s, CH_3); 69.03(s, CH_2); 83.07(s, C_5H_5); 121.40(d, *m*-C_6H_5); 125.23(d, *o*-C_6H_5); 129.71(d, C_6H_5); 218.05, 219.50(s, CO, CS).

Synthesis of η^5-C_5Me_5*Fe(CO)(*η^1*-SC(S)OEt)(PBu*$_3$*)* (**6a**). A solution of η^5-$C_5Me_5Fe(CO)_2$(η^1-SC(S)OEt) (**2**) (0.5g, 1.4 mmol) in 40 ml of degassed n-heptane was kept at 35 °C, until the solid had dissolved. To the red solution was added tri-n-butylphosphine (0.6 g, 3.0 mmol), and the temperature was raised to 85–90 °C. Monitoring by IR spectroscopy showed that the ν(CO) bands at 2020 and 1977 cm^{-1} due to complex **2** gradually diminished and gave way to new lower ν(CO) bands (1941w, sh, 1939vs, cm^{-1}). After 10 h at 85–90 °C, the reaction was complete, being the initial 2020 and 1977 cm^{-1} bands having completely disappeared. The solvent was removed in vacuo and the residue chromatographed. Elution with cyclohexane gave a brown band followed by a larger orange-red band. The solution from the brown band was evaporated in vacuo to give a brown solid (15%) which was identified as the bidentate xanthate complex η^5-C_5Me_5Fe(CO)(η^2-S_2COEt) (**4**), from its analysis and IR, and ^{1}H and ^{13}C NMR data, (see ref. [3]). The solution of the orange-red band was concentrated to 10 ml, then cooled, to give **6a** as red-orange crystals in 60% yield. ^{1}H NMR (δ (ppm), $CDCl_3$): 1.3–1.80(m, br, (CH_3), $(CH_3)_5$); 4.65(q, H, CH_2). ^{13}C NMR (δ (ppm), $CDCl_3$): 9.30(s, $(CH_3)_5$); 13.65, 14.10(s, CH_3); 25.10(d), 26.00(s), 26.85(d)(CH_2); 68.45(s, CH_2); 96.00(s, C_5), 217.10, 218.30(s, CO, CS).

6c: ^{1}H NMR (δ (ppm), $CDCl_3$): 1.20–1.58(m, br, $(CH_3)_5$, CH_3); 4.05–4.20(m, br, CH_2); ^{13}C NMR (δ (ppm), $CDCl_3$): 9.25(s, $(CH_3)_5$); 13.80(s, CH_3); 15.10(d, CH_3, *J*(PC) 7.0Hz); 60.85(d, CH_2, *J*(PC) 6.1Hz); 68.30(s, CH_2); 96.30(s, C_5); 216.70, 218.00(s, CO, CS).

6d: ^{1}H NMR (δ (ppm), $CDCl_3$): 1.30–1.55(m, br, $(CH_3)_5$, CH_3); 4.48(q, H, CH_2); 7.45(m, 15H, C_6H_5). ^{13}C NMR (δ (ppm), $CDCl_3$): 9.30(s, $(CH_3)_5$; 12.90(s, CH_3); 68.60(d, CH_2); 95.85(s, C_5); 120.34(d, *m*-C_6H_5); 124.55 6d, *o*-C_6H_5); 128.35(d, *p*-C_6H_5); 215.60, 214.00(s, CO, CS).

Synthesis of η^5-C_5H_5*Fe(*η^2*-*S_2*COEt)(PBu*$_3$*)* (**7a**). A degassed and stirred cyclohexane solution of **5a** (0.5 g, 1.1 mmol) was irradiated (UV light), at 40 ° C, and the reaction was monitored by IR spectroscopy. The initial ν(CO) band (1954vs, 1968 $\mathrm{cm^{-1}}$ sh), had disappeared completely after 1 h. The violet solution was filtered and subjected to chromatography, which gave a single violet band. The solvent was removed in vacuo to leave compound **7a** as a violet air-sensitive solid ^{1}H NMR (δ (ppm), $CDCl_3$) 1.55(t, 3H, CH_3); 1.30–1.45(m, br, 6H, CH_3); 4.50(q, CH_2); 4.98(s, 5H, C_5H_5); ^{13}C NMR (δ (ppm), $CDCl_3$): 13.10(s, CH_3); 13.90(s, CH_3); 23.50(d), 26.75(d), 27.95(d)(CH_2); 68.55(s, CH_2); 83.50(s, C_5H_5).

7b: ^{1}H NMR (δ (ppm), $CDCl_3$): 1.53(t, 3H, CH_3); 4.65(m, br, CH_2); 5.10(s, 5H, C_5H_5); 7.48(m, br, 15H, C_6H_5). ^{13}C NMR (δ (ppm), $CDCl_3$): 13.98(s, CH_3) 68.96(s, CH_2); 83.95(s, C_5H_5); 124.95(d, *m*-C_6H_5); 126.50(d, *o*-C_6H_5); 129.30(d, *p*-C_6H_5).

7c: ^{1}H NMR (δ (ppm), $CDCl_3$): 1.54(m, 6H, CH_3); 4.55(m, 4H, CH_2); 5.10(s, 5H, C_5H_5). ^{13}C NMR (δ (ppm), $CDCl_3$): 13.90(s, CH_3); 17.75(d, CH_3); 65.30(d, CH_2); 69.00(s, CH_2); 84.50(s, C_5H_5).

7d: ^{1}H NMR (δ (ppm), $CDCl_3$): 1.51(t, 3H, CH_3); 4.65(d, 2H, CH_2); 5.15(s, 5H, C_5H_5); 7.45(m, 15H, C_6H_5). ^{13}C NMR (δ (ppm), $CDCl_3$): 14.106(s, CH_3); 67.00(d, CH_2); 84.90(s, C_5H_5); 121.70(d, *o*-C_6H_5); 124.95(d, *m*-C_6H_5); 129.50(d, *p*-C_6H_5).

8a: ^{1}H NMR (δ (ppm), $CDCl_3$): 1.35–1.60(m, br, $(CH_3)_5$, CH_3); 4.69(m, H, CH_2); ^{13}C NMR (δ (ppm), $CDCl_3$): 9.28(s, $(CH_3)_5$); 13.90(s, CH_3); 25.15(d), 26.75(d), 27.00(d) (CH_2); 68.10(s, CH_2); 96.10(s, C_5).

8c: ^{1}H NMR (δ (ppm), $CDCl_3$): 1.28–1.55(m, br, $(CH_3)_5$, CH_3); 4.10–4.30(m, br, CH_2); ^{13}C NMR (δ (ppm), $CDCl_3$): 9.25(s, $(CH_3)_5$); 13.50(s, CH_3); 15.50(d, CH_3); 60.55(d, CH_2); 68.70(d, CH_2); 96.50(s, C_5).

8d: ^{1}H NMR (δ (ppm), $CDCl_3$): 1.35–1.60(m, br, $(CH_3)_5$, CH_3); 4.25(q, H, CH_2); 7.60(m, 15H, C_6H_5). ^{13}C NMR (δ (ppm), $CDCl_3$): 9.32(s, $(CH_3)_5$); 13.05(s, (CH_3); 68.75(d, CH_2); 96.10(s, C_5); 121.50(d, *o*-C_6H_5); 125.60(d, *m*-C_6H_5); 129.30(d, *p*-C_6H_5).

Acknowledgements

We thank the CAICYT (Spain) for financial support of this work, and BASF AG (Ludwigshafen) for a generous gift of $Fe(CO)_5$.

References

1 M. Morán and I. Cuadrado, J. Organomet. Chem. 295 (1985) 353.
2 M. Morán and I. Cuadrado, J. Organomet. Chem., 311 (1986) 333.
3 M. Morán, I. Cuadrado, C. Muñoz-Reja, J.R. Masaguer and J. Losada, J. Chem. Soc. Dalton, Trans., in press.
4 This different behaviour has been reported for other pentamethylcyclopentadienyliron complexes, see (a) D. Astruc, Tetrahedron, 39 (1983) 4027 (report No. 157); (b) D. Catheline and D. Astruc, Organometallics, 3 (1984) 1094.
5 C.A. Tolman, Chem. Rev., 77 (1977) 313.
6 C.E. Davies, I.M. Gardiner. M.L.H. Green, N.J. Hazel, P.D. Grebenick, V.S.B. Metwa, K. Prout, J. Chem. Soc. Dalton Trans., (1985) 669.
7 D. Catheline, E. Román and D. Astruc, Inorg. Chem., 23 (1984) 4058.
8 (a) E. Román, D. Catheline and D. Astruc, J. Organomet. Chem., 236 (1982) 229; (b) D. Astruc, Acc. Chem. Res., 12 (1986) 377; (c) D. Catheline and D. Astruc, Coord. Chem., 23 (1982) 41.
9 M.L. Shankaranarayana and C.C. Patel, Spectrochim. Acta, 21 (1965) 229.

10 U. Argarwala, P.B. Rao, Inorg. Chim. Acta, 2 (1968) 337.

11 G.W. Watt, and B.J. McCormick, Spectrochim. Acta, 21 (1965) 753.

12 O.P. Pandey, S.K. Sengupta and S.C. Tripathi, Polyhedron, 3 (1984) 695.

13 R.S.P. Coutts, P.C. Wailes and J.V. Kingston, Aust. J. Chem. 23 (1970) 469.

14 D.A. Brown, H.J. Lyons and R.A. Manning, Inorg. Chim. Acta, 4 (1970) 428.

15 R.B. King, R.N. Kapoor and K.H. Pannel, J. Organomet. Chem., 20 (1969) 187.

16 R.B. King, L.W. Houk and K.H. Pannel, Inorg. Chem., 8 (1969) 1042.

17 R.B. King, Inorg. Chim. Acta, 2 (1968) 454.

18 O.A. Gansow, D.A. Schexnayder, B.J. Kimura, J. Am. Chem. Soc., 94 (1972) 3406.

19 C.A. Tolman, J. Am. Chem. Soc., 92 (1970) 2953, 2956.

20 F.A. Cotton and C.S. Kraihanzel, J. Am. Chem. Soc., 84 (1962) 4432.

21 Some cyclopentadienyliron complexes give stable cations, [22–24].

22 P.M. Treichel, K.P. Wagner and H.J. Much, J. Organomet. Chem. 86 (1975) C13.

23 P.M. Treichel, D.C. Molzahn and K.P. Wagner, J. Organomet. Chem., 174 (1979) 191.

24 P.M. Treichel, and D.A. Komar, J. Organomet. Chem., 206 (1981) 77.

25 Attempts are in progress to isolate these cations with xanthate ligands and other bidentate sulphur-containing ligands.

26 In our work this peak also appeared in the irreversible oxidation of η^5-$C_5R_5Fe(CO)LI$ compounds ($L = P(OEt)_3$ or $P(OPh)_3$).

27 D.L. Reger and C.J. Coleman, Inorg. Chem., 18 (1979) 3155.